17th World Conference on Earthquake Engineering, 17WCEE
Sendai, Japan - September 13th to 18th 2020

OPTIMIZING THE INTEGRATED STRUCTURAL AND NONSTRUCTURAL SEISMIC RETROFIT OF BUILDINGS

P. Steneker[(1)], A. Filiatrault[(2)(3)], L. Wiebe[(4)], D. Konstantinidis[(5)]

[(1)] *Graduate Student, Department of Civil Engineering, McMaster University, stenekpr@mcmaster.ca*
[(2)] *Professor, University School for Advanced Studies IUSS, Pavia, andre.filiatrault@iusspavia.it*
[(3)] *Professor, Department of Civil, Structural and Environmental Engineering, University at Buffalo State University of New York af36@buffalo.edu*
[(4)] *Associate Professor, Department of Civil Engineering, McMaster University, wiebel@mcmaster.ca*
[(5)] *Assistant Professor, Department of Civil and Environmental Engineering, University of California, Berkeley, konstantinidis@berkeley.edu*

Abstract

A key component in the performance-based seismic design or retrofit of buildings is the assessment of anticipated losses from damage to structural and nonstructural components. Currently these anticipated losses are estimated using performance-based seismic loss procedures that are building case specific, as embodied in the Performance-Based Earthquake Engineering (PBEE) framework developed by the Pacific Earthquake Engineering Research (PEER) Center. As these procedures do not easily allow for the integrated optimization of structural and nonstructural interventions in a particular building, a general optimization procedure within the PBEE framework and implemented through the FEMA P-58 methodology has been developed and is discussed in this paper.

This paper begins with a short description of the proposed optimization procedure, implemented with the use of a genetic algorithm, which considers integrated structural and nonstructural seismic retrofits. A case study archetype building is used to demonstrate the application of the optimization procedure using one economic target metric considered in the PEER-PBEE framework. The results of the case study demonstrate how this optimization process quickly and reliably converges to different allocations of resources for structural and nonstructural retrofits, depending on the owner specific expectations, such as expected rate of return and occupancy time. Using the genetic algorithm framework, a range of optimum retrofit solutions are developed for the specific archetype structure considered, based on a range of owner expectations. The trends offered by these suites of optimum retrofit solutions provide guidance on identifying the optimal allocation of resources for buildings with similar properties.

Keywords: Performance-Based Earthquake Engineering; FEMA P-58; Cost-Benefit Analysis; Seismic Losses; Genetic Algorithm; Design Optimization; Nonstructural Components

1. Introduction

The development of the Performance-Based Earthquake Engineering (PBEE) framework by the Pacific Earthquake Engineering Research Center (PEER) [1-3] and its implementation through the FEMA P-58 methodology [4] provide designers and building owners with tools to describe the seismic performance of building systems, including both structural and nonstructural components. The PEER-PBEE framework includes four stages, with hazard analysis, structural analysis, and damage analysis being conducted to provide information for a final loss analysis, which determines decision variables. The importance of considering both structural and nonstructural seismic losses in a seismic design or retrofit situation is now recognized and has been discussed extensively in the last decades [5-7]. More recently, procedures to conduct cost-benefit analyses to reduce economic losses have been developed [8, 9].

The PEER-PBEE framework targets a specific building case, thereby limiting the selection of a seismic retrofit strategy to a trial-and-error approach, since the selection of any single component (structural or nonstructural) retrofit must be considered within the context of a full system-level analysis. This is typically aided by some guidance from experienced designers. This building case specific approach does not easily allow the optimization of integrated structural/nonstructural interventions. Only a few studies have considered optimization procedures for the seismic design or retrofit of buildings. Most of these strategies involved the use of genetic algorithms as an optimization process implemented within the PEER-PBEE framework as it consists of a stochastic optimization solution. So far, however, these strategies were limited in scope to structural design decisions [10-16]. None of the previous optimization studies listed above included a process to determine the optimal resource allocation between structural and nonstructural retrofits with the purpose of minimizing seismic losses.

The results obtained from such an optimization process could be used by building owners and non-engineering professionals to better conduct investment planning and risk mitigation analysis for their asset's life cycle. The main objective of this study is to introduce such an optimization framework, consistent with the PEER-PBEE framework. A case study structure, using economic loss as the target optimization metric, is used to provide an example of the framework's implementation. The case study includes the optimization of four different structural retrofit strategies, each considered independently but in combination with nonstructural retrofits, to a three-story steel moment-resisting frame (MRF) with an office type occupancy. Since each structural retrofit strategy has a distinct impact on the engineering demand parameters (EDPs) at each floor level, the consideration of a particular structural retrofit has an impact on the types of nonstructural components selected for retrofit.

2. Overview of Genetic Algorithm and Implementation in the PEER-PBEE Framework

The genetic algorithm is based on the principles of evolutionary biology and has been applied to various areas of engineering [17, 18]. It replicates natural evolutionary selection theory with the use of repetitive iterations, where individuals within a population who have a higher fitness have a higher degree of propagation to the following generation. Both probabilistic-based crossovers of individuals forming the next generation and random mutations are used to ensure some population diversity as the algorithm converges towards an optimal solution.

The development of a genetic algorithm can be summarized into five main steps: 1) the formulation of the genetic code defining each individual within the population; 2) the evaluation of the performance of each individual using a ranking function for a specific target metric; 3) the selection and mixing of individuals to form a new generation seeking higher performing individuals; 4) the mutation of individuals to ensure genetic diversity; and 5) the determination of an optimum solution using single or multiple convergence criteria. These five steps are highlighted in Fig. 1, which summarizes also the implementation of the genetic algorithm within the PEER-PBEE framework.

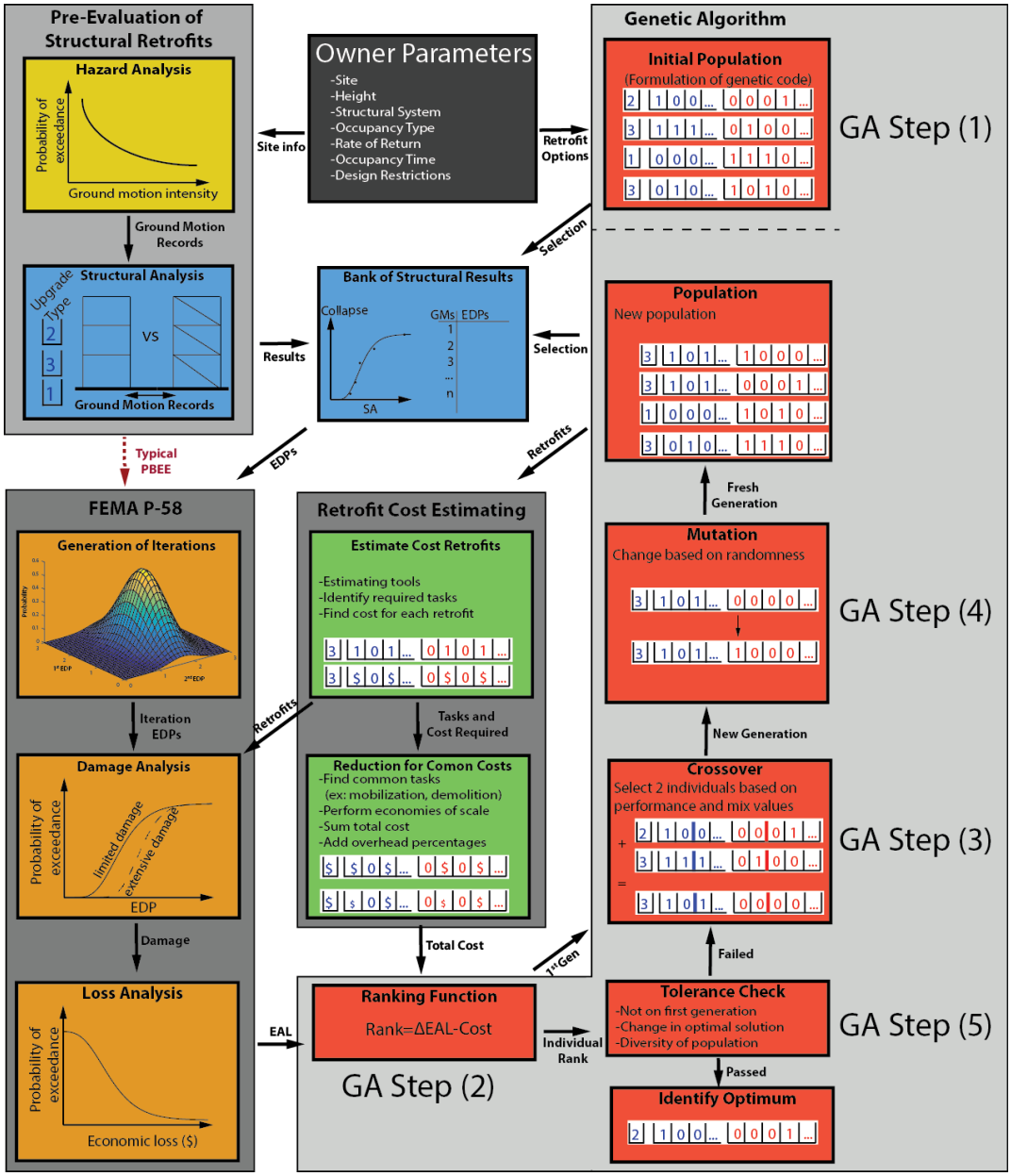

Fig. 1 – Flow chart for optimization methodology

The process begins with the identification of the building owner parameters. The components of the genetic algorithm must be adapted to ensure that all considered retrofit options are evaluated within the PEER-PBEE framework. Implementing the PEER-PBEE framework requires the formulation of the genetic code (i.e. string of bits) of each individual within the population with a sufficient number of bits to represent each component's retrofit, forming Step (1) of Fig. 1. As shown in Fig. 2, each nonstructural component is represented with its own binary bit, where a zero bit represents a non-retrofitted status, and a unity bit represents a retrofitted status. Each retrofitted nonstructural component is based on retrofit interventions proposed in FEMA E-74 [19] and is accompanied by an improvement of its fragility curves, as defined in FEMA P-58 [5]. The identification of a particular structural retrofit strategy is made by two sets of bits. The value of the first "Structural" retrofit option bit varies from unity to N (see Fig. 2), where N is the maximum number of structural retrofit strategies being considered. The implementation of the structural retrofit strategy is then represented by one structural retrofit implementation binary bit for each floor of the building (with a value of unity indicating a retrofit at that floor). This procedure provides more flexibility to structural retrofits

on a floor-by-floor basis, rather than limiting the decision to the entire building at once. The introduction of a particular unity bit at a given floor requires nonlinear time history analyses conducted at multiple intensity stripes both to generate the collapse fragility curve of the retrofitted building and to determine the values of the EDPs for each floor, which are needed to evaluate the nonstructural damage from the initial or retrofitted fragility curves. The string of an individual could be constructed for any number of different structural retrofit types (N) or building floors and could consider any number of nonstructural components desired. Furthermore, the optimization procedure allows for the possible inclusions of component or system level constraints.

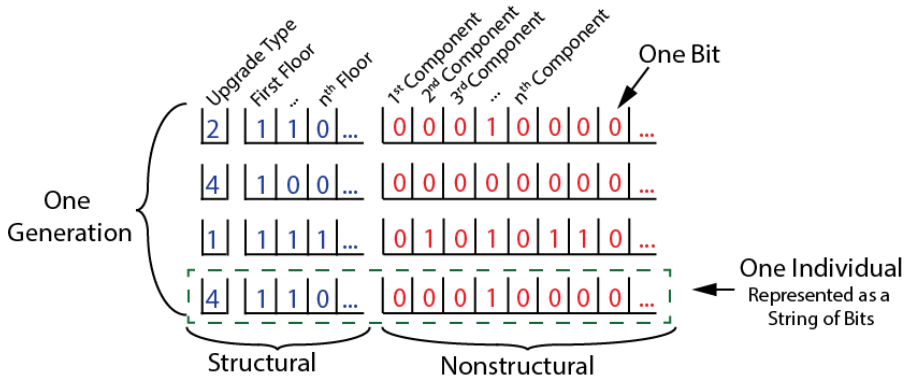

Fig. 2 – Example of population formulation in genetic algorithm

Following the formation of the genetic code of the individuals of the initial population, the fitness of each individual within a population is evaluated and ranked using a ranking function for each target metric considered, identified as Step (2) in Fig. 1. The target metric considered in this study is an economic target metric, which compares the total cost of each integrated structural and nonstructural retrofit strategy to the benefits derived from a reduction of seismically induced economic loss over the occupancy time. The ranking function ($Rank_{Economic}$) associated with this economic target metric is given by:

$$Rank_{Economic} = \frac{EAL_O - EAL_U}{R}\left(1 - \frac{1}{(1+R)^t}\right) - UC \quad (1)$$

where EAL_O is the estimated annual loss of the original (non-retrofitted) building, EAL_U is the estimated annual loss of the retrofit scenario being considered under evaluation (i.e. an individual in a generation), R is the annual internal rate of return expected by the owner, t is the expected occupancy time of the building in years, and UC is the total cost of the combination of chosen retrofits. A positive rank for an individual indicates that the economic gain due to the risk reduction outweighs the retrofit cost. Therefore, maximizing the positive rank represents the optimal design objective for the economic target metric.

The initial population described above is formed by individuals having randomly assigned bit values. This provides an initial diversity to the population before the selective optimizing begins. After the fitness of each individual is evaluated and ranked, a crossover is conducted (Step (3) in Fig. 1), where two individuals are randomly selected with a weighted preference according to their rank. The strings of these highly ranked individuals are spliced and mixed to form a new generation of the same population size as the previous generation. A carryover percentage is used to guarantee the existence of a certain number of the best performing individuals from the previous generation moving into the next generation without undergoing splicing.

Once the new generation is formed, each bit can mutate based on a pre-determined mutation rate (Step (4) in Fig. 1). If a bit mutates, its value is randomly reassigned using a uniform distribution. The new generation is then evaluated and ranked again. The optimization process is deemed to have reached a solution once a set of convergence criteria is satisfied (Step 5 in Fig. 1). Finally, since the genetic algorithm is a heuristic searching algorithm, multiple algorithm runs are needed to increase the confidence in the solution obtained for each target metric. Further details are found in Steneker et al. [20].

3. Retrofit Case Study

A retrofit case study was developed to demonstrate the capabilities of the genetic algorithm optimization process in influencing decision-making within the PEER-PBEE framework. An archetype building was selected, and several owner-specific parameters were defined in terms of internal rate of return (R) and building occupancy time (t).

3.1 Archetype Building

The original (non-retrofitted) archetype building in this case study is an existing three-story office type building [21, 22], to be retrofitted in Seattle, Washington. The seismic force-resisting system is composed of perimeter steel MRFs with pre-Northridge Earthquake beam-to-column connections. Each archetype frame was designed according to the seismic provisions of the 1994 Uniform Building Code [23] for a Site Class B. With the exception of the use of pre-Northridge connections, each archetype frame satisfies current ASCE 7-16 [24] and AISC 341-16 seismic design requirements [25]. The computed fundamental period of each MRF with assigned tributary seismic weight (see Fig. 3) is 0.87 s. The frame model was assembled in the OpenSees software [26] and consisted of elastic beam-to-column elements with concentrated rotational plastic hinges, using the Ibarra-Medina-Krawinkler model [27] at the element ends. Each beam-to-column joint was modeled to capture panel zone yielding using the Krawinkler Spring Box model illustrated in Fig. 3(a) [21], and was modeled using a trilinear backbone curve [28]. The building was assumed to have no irregularities causing torsional effects and, thus, its seismic response was obtained independently by analyzing one MRF in the North-South and East-West directions. Rayleigh damping of 2% was applied to each frame in the first and second elastic modes, mirroring common modeling practice.

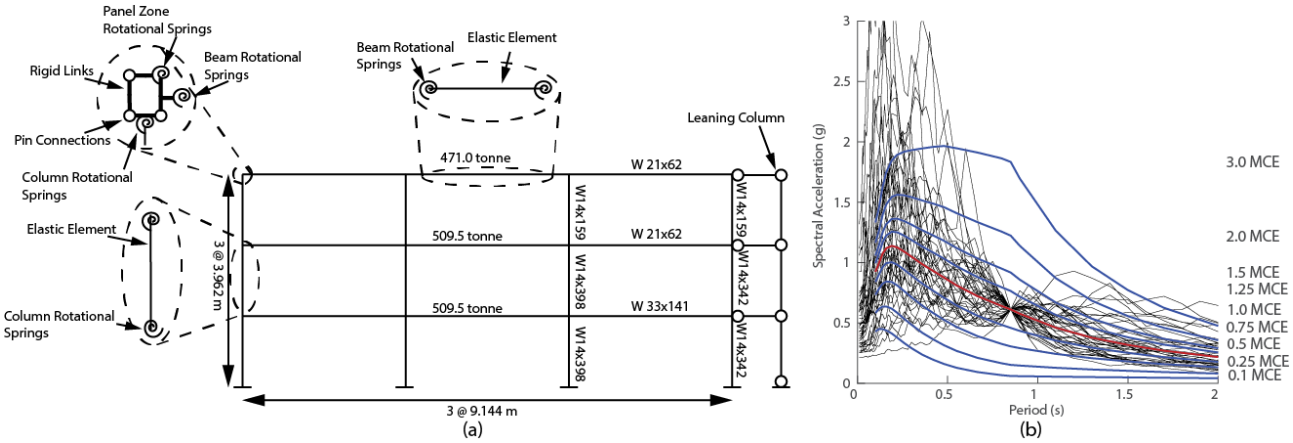

Fig. 3 – (a) Elevation view and modeling details of seismic force-resisting system of three-story steel office type archetype building, (b) Conditional spectra for archetype building

The collapse performance of the archetype frame was evaluated by a multiple stripe analyses using nine intensity stripes [29]. For each stripe, 40 ground motion component pairs were selected and scaled to match a conditional spectrum with a target spectral acceleration at the first-mode period of the building [30]. The ground motions were selected from the far-field NGA-West2 Database [31]. The conditional spectrum for each stripe, as well as the spectrum for each of the 40 ground motions selected at a risk-based maximum considered earthquake (MCE_R) intensity level (2475 years return period) for the building site, are shown in Fig. 3 (b).

3.2 Structural Retrofits

Four structural retrofit options were considered in this case study, all selected with a goal of reducing structural damage. The design of each option was performed considering an implementation at any combination of floors. The first option consisted of replacing the pre-Northridge moment resisting connections of the archetype frame with newly developed self-centering sliding hinge joint connections (SCSHJ) [32, 33]. This type of connection dissipates energy using a sliding interface instead of relying on deformations within

the beam-to-column connections. When coupled with a ring spring [34] above and/or below the beam flanges, this connection is able to self-center. The second structural retrofit strategy considered in this case study was the installation of diagonal buckling restrained braces (BRB) [35] across a bay opening within the frame. These braces were designed to replace the MRF as the seismic force-resisting system of the building, while the existing MRF became a secondary system. The third and fourth retrofit options consisted of the installation of linear viscous dampers [36] diagonally across a bay opening within the frame. The targeted first modal viscous damping ratios were 10% and 25% of critical for the second and third retrofit options, respectively. A summary of the designs of these four structural retrofit strategies for each floor of the archetype building is provided in Table 1.

Table 1 – Summary of structural retrofit implementations per frame in each floor of archetype building

Floor number	**Self-Centering Sliding Hinge Joints at each MRF Connection** (100% Self-Centering Ratio) Activation Moments:	**Buckling Restrained Braces** (Yield Strength: 350 MPa) Cross-Sectional Area:	**Linear Viscous Dampers (10% first modal damping)** Damping coefficient:	**Linear Viscous Dampers (25% first modal damping)** Damping coefficient:
1	$M_{y\ beam}/3$=709 kN·m	4,300 mm^2	7,400 kN·s/m	19,500 kN·s/m
2	$M_{y\ beam}/3$=201 kN·m	2,800 mm^2	3,900 kN·s/m	10,200 kN·s/m
3	$M_{y\ beam}/3$=201 kN·m	2,800 mm^2	1,270 kN·s/m	3,300 kN·s/m

Note: $M_{y,\ beam}$ = Yield moment of beam

3.3 Nonstructural Retrofits

The nonstructural components included in the archetype building and considered in the loss estimation analysis are those identified in FEMA P-58 3.3 "*Normative Quantity Estimating Tool"* [21] for the archetype office occupancy type and are listed in Table 2. These consist of 26 nonstructural component typologies, with each having an as-is (unretrofitted) fragility curve and a seismically retrofitted fragility curve, whose values are specified in the FEMA P-58 component library for retrofit interventions that are consistent with those proposed in FEMA E-74. Where more recent nonstructural research results were identified, the associated fragility curves for some of the nonstructural components were updated as identified in the available references. The only consequence functions that were modified were for the piping systems, where the consequence function for an additional component (C3021.001a: Generic Floor Covering - Flooding of floor caused by failure of pipe - Office - Dry) was added to include water damage to surrounding flooring based on estimated affected areas. These areas were determined using both the description of damage in FEMA P-58 and the pipe sizes, where small leaks and smaller diameter pipe breaks caused only a fraction of floor area to be damaged in comparison to breaks in large diameter pipes.

4. Structural Retrofit Performance

In order to provide an initial understanding of the impact of each structural retrofit on the overall optimal structural/nonstructural retrofit strategy, a summary of the probability of exceeding threshold values for three different EDPs at three different performance objectives are shown in Fig. 4 for all structural retrofit scenarios implemented at all three floors. The three EDPs used are considered for loss estimation in FEMA P-58 [4] and are the peak interstory drift, the peak residual interstory drift, and the peak floor acceleration. The performance objectives were taken from ASCE 41 [42] and are: immediate occupancy/position retention, life safety, and collapse prevention/hazard reduction. The threshold drift values used were derived from Table C2-4 of ASCE 41 for steel MRF beam rotation values using pre-Northridge connections, while the acceleration values were determined based on the median accelerations of the corresponding damage state fragility curves of various nonstructural office components defined in FEMA P-58 [4] based on the damage definitions in ASCE 41 [42]. However, the acceleration values used in this study are only reference values for illustrative comparisons and do not indicate distinct thresholds of damage, which are highly variable between different nonstructural components.

Table 2 – List of Nonstructural Components in Archetype Building

Component Category							
Mechanical Equipment	Chiller	Cooling Tower	Air Handling Unit	Motor Controller	Low Voltage Transformer	Distribution Panel	Control Panel
Plumbing	Cold Piping	Large Diam. Piping	Small Diam. Piping	Sanitary Piping	Sprinkler Piping [37]	Sprinkler Head [37]	
Contents	Lighting	Desktop Equipment	Office Furniture [38]				
Finishes	Suspended Ceiling	Raised Floor	Curtain Glazing [39]	Wall Partitions [40]	Roofing Tile		
HVAC	Large HVAC	Small HVAC Duct	HVAC Diffuser				
Egress	Stairs [41]	Elevator					

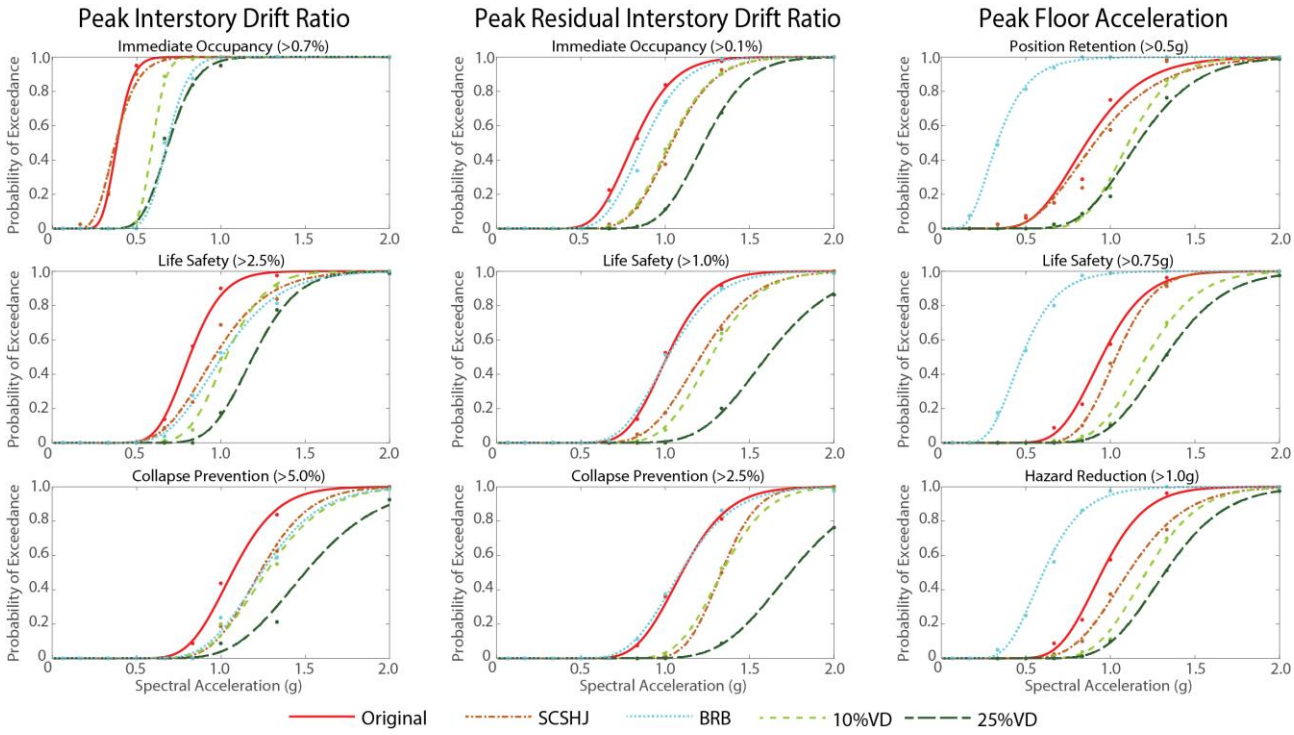

Fig. 4 – Summary of structural performances of retrofits

The impact of each structural retrofit strategy on the collapse performance of the structure is indicated by the change in collapse prevention, measured using the inter-story drift EDP, found in the bottom left of Fig. 4. The collapse margin ratio (CMR), defined as the ratio between the median collapse capacity to the MCE_R spectral intensity, of the original building is 1.5, and is improved to 1.85 with the SCSHJ retrofit option, 1.86 for the BRB, 1.9 for the 10%VD and 2.25 for the 25%VD. The improvement of the CMR at this performance level reduces the estimated losses, as it lowers the contribution of the building collapse to the EAL. For the life safety performance level, a similar overall percentage of improvement of the margin ratio (MR, calculated by dividing the EDP value at the median probability of exceedance by the MCE value) is observed. However, the improvement in MR is not maintained at the immediate occupancy performance level, where the MR of the original structure and the SCSHJ retrofit is 0.58, the MR for the 10%VD is 0.9, and the MR for the BRB

and 25%VD is 1.03. The less significant improvement in MR at the immediate occupancy performance level is important since many of the drift sensitive nonstructural components experience damage at drifts between the immediate occupancy and life safety threshold values. The effects will be discussed in section 5.2.

When examining residual interstory drifts, the changes in performance impacts the total building loss due to it being tagged as unsafe. The same trends in performance are observed across all three performance objectives, where the BRB did not improve the performance, the 10%VD and SCSHJ retrofits improved the performance by increasing the MR by 20%, and the 25%VD had the highest improvement in MR by more than 50%.

For the acceleration EDP at all three performance objectives, the addition of BRBs decreases the performance by more than 100%, identifying this retrofit option as potentially increasing the damage to acceleration-sensitive nonstructural components. The performance of the SCSHJ retrofit improved with higher seismic intensities, as the connections had a lower activation moment than the pre-Northridge connections, and therefore could dissipate more energy at larger intensities. Finally, the 10% and 25%VD retrofits improved the MR by 30% and 40%, respectively, at all performance objectives. The reduction in floor accelerations provided by the addition of viscous dampers will reduce the losses to acceleration-sensitive nonstructural components, further encouraging the selection of viscous dampers in the optimization methodology.

5. Optimization Process

After the results from the nonlinear time history analysis had been compiled, the genetic algorithm optimization methodology was conducted for each of the four structural options by locking the "structural retrofit option" bit to the corresponding value. The optimization was conducted for 16 different combinations of rate of return and occupancy time values. The rates of return (R) used were 2%, 6%, 10%, and 15%, while the occupancy times (t) used were 10 years, 30 years, 50 years, and 70 years. Each run of the optimization methodology was continued until convergence was achieved on an optimal solution. A carryover percentage of 10% was used to pass the top performing individuals into the next generation and a mutation rate of 2% was used for all runs. Two simultaneous convergence criteria were used to define an optimized solution: 1) a change of less than 1% in the rank of the optimal solution (individual) between the current and the previous generation and, 2) the population of the current generation consists of at least 25% of individuals having the highest ranked genetic code (i.e. 25% of optimal individuals).

5.1 Example of Optimization Runs

Two optimization runs are used to illustrate the variability of results obtained in the matrix of 16 owner R and t values, as shown in Fig. 5. Each run used the 25% viscous damper structural retrofit. The first run had as owner parameters a rate of return R = 2% and an occupancy time t = 70 years, representative of a long-term institutional owner, such as a government entity targeting value-added real estate returns typical of the Western United States [43]. The second run had for owner parameters R = 15% and t = 10 years, representing a short-term owner with a higher acceptable risk level, such as a real-estate investor/developer. The results of the fitting function for each individual of each generation for both runs are shown in Fig. 5 (a) for the long-term owner, and Fig 5. (b) for the short-term owner. The optimal solution are identified, as well as the rank for the original building (with no retrofit cost and therefore no change in EAL), and for the building with all nonstructural retrofits implemented, which was forcibly included in each generation by locking all nonstructural bits to a value of one. The fully retrofitted structure has a *Rank* value lower than the optimal solution since some of the retrofit options provided a reduction in net present value of EAL that was less than their capital implementation, even at low rates and long occupancy times. Finally, the optimal retrofit strategy is shown in Fig. 5 (c) and (d) for the long-term and short-term owners, respectively. Since both the processes to obtain the EAL, as outlined in FEMA P-58, and the retrofit cost have some degrees of variability, the calculated *Rank* for two identical individuals can vary slightly. This is seen as changes in Rank values obtained for identical individuals, such as the locked values of the fully retrofitted strategy, across multiple generations.

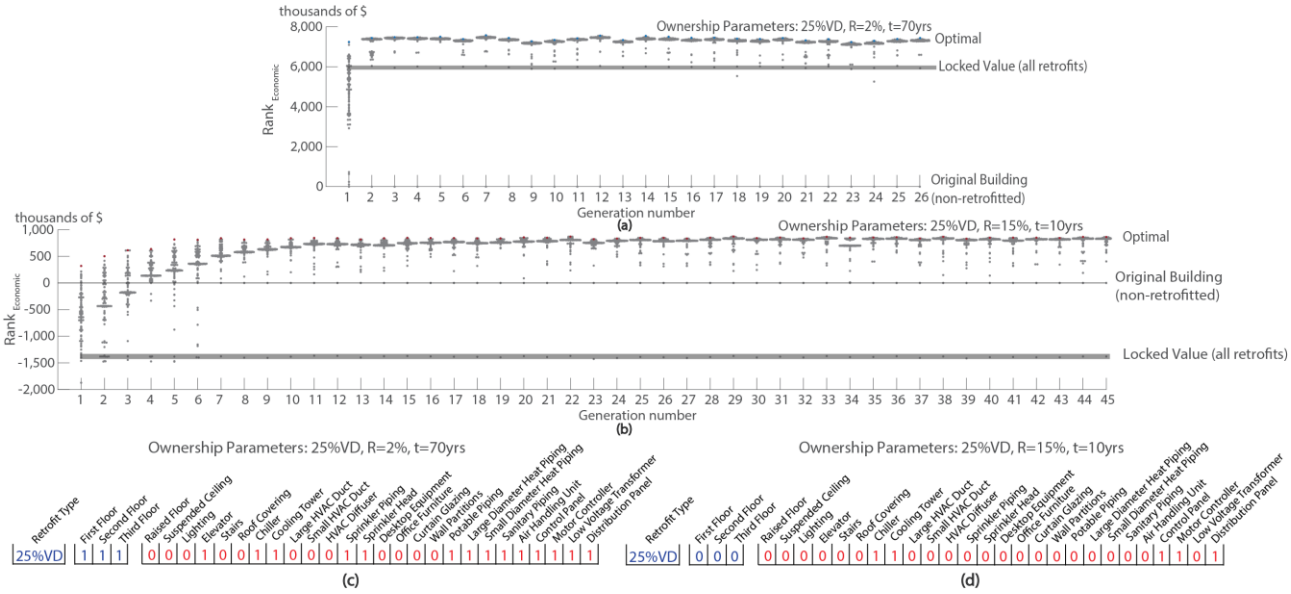

Fig. 5 – (a) Genetic algorithm run for *R*=2%, *t*=70yrs, (b) Genetic algorithm run for *R*=15%, *t*=10yrs, (c) and (d) Optimal solutions for (a) and (b), respectively

5.2 Summary of Optimal Results

The use of a particular structural retrofit strategy resulted in differences in the overall optimal retrofit scheme. The first row of Fig. 6 first summarizes the optimal retrofit cost for each of the four structural retrofit strategies, as a percentage of the total building value, for the four considered rates of return and four occupancy times. Each optimal retrofit cost is a summation of all of the retrofit strategies determined by the methodology, and corresponds to a decrease in the EAL, shown in the second row of Fig. 6. Finally, the breakdown of cost directed to the structural of nonstructural retrofit is shown in the third row of Fig. 6 for each of the four structural retrofit strategies and the 16 different combinations of owner parameters.

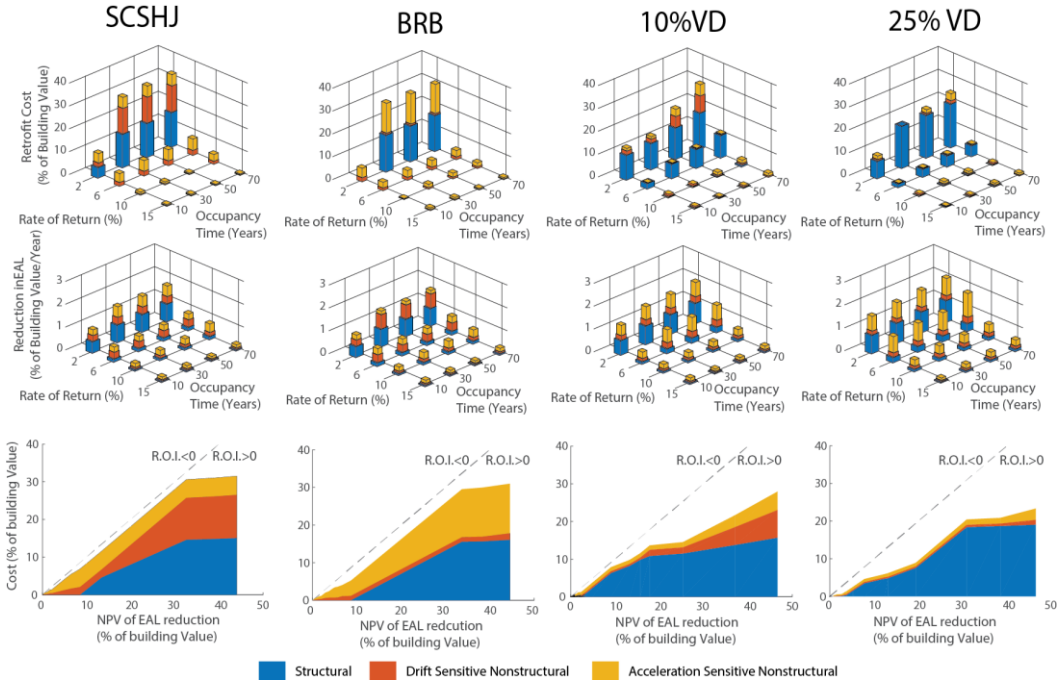

Fig. 6 – (top) Optimum retrofit scheme cost vs rate of return and occupancy time, (middle) Reduction in EAL vs rate of return and occupancy time, (bottom) breakdown of retrofit cost vs NPV reduction

The retrofit cost and EAL values obtained at a rate of return of 2% and occupancy time of 70 years provides a reference point for comparison across the structural retrofit strategies. For these owner parameters, the 25% viscous damping structural retrofit has the best overall optimization rank, as it has the lowest overall retrofit cost, only 24% of the building value, corresponding to the largest reduction in EAL of 2.02% of the building value per year, when compared to the other three strategies. The 10% viscous damping option exhibits a slightly inferior performance, having a retrofit cost of 28% and a reduction in EAL of 1.98%. Finally, both the SCSHJ connection retrofit strategy, and the BRB retrofit strategy have smaller reductions in EAL at 1.55% of the building value, for comparatively higher retrofit costs of 31% and 30% of the building value, respectively. However, with owner parameters consisting of long occupancy times and small required rates of return, all four structural retrofit strategies will provide a more advantageous reduction in losses when compared to their capital investment costs. Even the BRB strategy, which increased the peak floor accelerations, provided an adequate increase in the collapse performance of the structure to justify both its initial expense and the resulting increase in potential for damage to acceleration-sensitive nonstructural components. However, this is not the case when examining owner parameters with higher rates of return and/or lower occupancy time, as discussed further below.

The last row in Figure 6 compares the net present value of the reduction in EAL for each set of owner parameters against the total optimal capital investment cost as determined by the optimization methodology. The break-even function indicated by a rate of investment (ROI) of 0 is shown in each graph, where an ROI greater than 0 indicates an investment with a positive return. The major differences observed when comparing the results across each structural retrofit strategy stem directly from the analysis of the structural performances in the previous section. Mainly, the reduction in floor accelerations and interstory drifts provided by the viscous damping retrofit schemes allowed for a comparatively smaller quantity of nonstructural upgrading when compared to the SCSHJ or BRB structural retrofits. The larger and more expensive 25% damped viscous dampers required little investment in nonstructural retrofits, while the smaller, less expensive 10% damped viscous dampers required an increase in nonstructural investment that surpassed the savings in damper expense. For the BRB structural retrofit, a large expense in nonstructural retrofits was required because of the increase in floor accelerations caused both by the introduction of a stiffer structural system, and further structural resiliency to larger earthquake intensities. Similarly, the SCSHJ structural retrofit provided a significant increase in the collapse performance of the structure as discussed previously, and required significant investment in drift sensitive nonstructural components to fully exploit this gain. At a rate of return of 6% or higher, the SCSHJ or BRB retrofits were not selected for any considered occupancy time, and the investment was instead directed to further nonstructural retrofits in both cases. For the viscous damping retrofits, both strategies identified a limited implementation as being optimal at this rate, identifying the installation of viscous dampers at only a select number of floors within the building.

No structural retrofit was deemed economically optimal at rates of return higher than 6%, independent of the owner occupancy time. Therefore, at these higher rates of return, only the most advantageous nonstructural retrofits were selected and were identical across all four structural retrofit strategies. These retrofits mostly consisted of large mechanical equipment, such as chillers, cooling towers, controllers, electrical distribution and control panels. The cost of seismically upgrading these equipment items is relatively low (mostly consisting of reinstallation on isolators or added anchorage), and has the potential to be further reduced by taking advantage of economies of scale (primarily in regards to shared mobilization costs), while the cost of damage to these large equipment items due to low and moderate seismic activity can be very high. Retrofits to these nonstructural components should be considered as a priority for all owner parameters considered within the bounds of this analysis.

6. Conclusion

This paper presented a methodology for determining the optimal structural and nonstructural retrofits based on economic targets across various different owner parameters, such as variations in rate of return and occupancy times. A case study was presented for a three-story pre-Northridge steel moment resisting frame located in Seattle, Washington, with an office type occupancy, considering four different structural retrofits:

Self-Centering Sliding Hinge Connections, Buckling Restrained Braces (BRB), and viscous dampers targeting either 10% or 25% of critical supplemental damping in the first mode. Furthermore, 26 different nonstructural components were included for potential retrofit. An analysis of the optimal solution across different rates of return and occupancy times was conducted on each of the structural retrofit approaches to identify key differences in optimal retrofit strategies. The 25% viscous damping retrofit was identified as producing the optimal cost-benefit solutions at rates lower than 6%, and retrofits to most mechanical equipment were identified as optimal for all rates of return. The BRB structural retrofit, which increased floor accelerations, required a significantly larger investment in nonstructural retrofits to provide an overall reduction in estimated annual loss.

6. References

[1] Cornell, C. A., and Krawinkler, H. (2000): Progress and Challenges in Seismic Performance Assessment. *PEER News*, April.

[2] Miranda, E., and Aslani, H. (2003): Probabilistic Response Assessment for Building-Specific Loss Estimation. *PEER Report No. 2003/03*, Pacific Earthquake Engineering Research, CA.

[3] Moehle, J., and Deierlein, G. (2004): A Framework Methodology for Performance-Based Earthquake Engineering. *Proceedings of the 13th World Conference on Earthquake Engineering*, Vancouver, BC, Canada.

[4] FEMA (2012): Seismic Performance Assessment of Buildings - Methodology. *Report P-58 Federal Emergency Management Agency*, **1**, 1-278, Washington, D.C.

[5] Miranda, E., and Taghavi, S. (2003): Estimation of Seismic Demands on Acceleration-sensitive Nonstructural Components in Critical Facilities. *ATC-29-2 Report*, Applied Technology Council, CA.

[6] Bradley, B., Dhakal, R., Cubrinovski, M., MacRae, G., and Lee, D. (2009): Seismic Loss Estimation for Efficient Decision Making. *Bulletin of the New Zealand Society for Earthquake Engineering*, **42** (2), 96-110.

[7] Molina, C., Almufti, S., Wilford, M., and Deierlein, G. (2016): Seismic Loss and Downtime Assessment of Existing Tall Steel-Framed Buildings and Strategies for Increased Resilience. *Journal of Structural Engineering*, **142** (8).

[8] Hofer, L., Zanini, M., Faleschini, F., and Pellegrino, C. (2018): Profitability Analysis for Assessing the Optimal Seismic Retrofit Strategy of Industrial Productive Processes with Business-Interruption Consequences. *Journal of Structural Engineering*, **144** (2).

[9] Sousa, L., and Monteiro, R. (2018): Seismic Retrofit Options for Nonstructural Building Partition Walls: Impact on Loss Estimation and Cost-benefit Analysis. *Engineering Structures*, **161**, 8-27.

[10] Rojas, M., Foley, C., and Pezeshk, S. (2011): Risk-based Seismic Design for Optimal Structural and Nonstructural System Performance. *Earthquake Spectra*. **27** (3), 857-880.

[11] Apostolakis, G., Dargush, G., and Filiatrault, A. (2014): Computational Framework for Automated Seismic Design of Self-Centering Connections in Steel Frames. *Journal of Computing in Civil Engineering*, **28** (2), 170-181.

[12] Farhat, F., Nakamura, S., and Takahashi, K. (2009): Application of Genetic Algorithm to Optimization of Buckling Restrained Braces for Seismic Upgrading of Existing Structures. *Computers and Structures*, **87**, 110-119.

[13] Wongprasert, N., and Symans, D. (2004): Application of a Genetic Algorithm for Optimal Damper Distribution within the Nonlinear Seismic Benchmark Building. *Journal of Engineering Mechanics*, **130** (4), 401-406.

[14] Gidaris, I., and Taflanidis, A. (2015): Performance Assessment and Optimization of Fluid Viscous Dampers Through Life-cycle Cost Criteria and Comparison to Alternative Design Approaches. *Bulletin of Earthquake Engineering*, **13**, 1003-1028.

[15] Pollini, N., Lavan, O., and Amir, O. (2017): Minimum-Cost Optimization of Nonlinear Fluid Viscous Dampers and their Supporting Members for Seismic Retrofitting. *Earthquake Engineering and Structural Dynamics*, **46**, 1941-1961.

[16] Pollini, N., Lavan, O., and Amir, O. (2018): Optimization-Based Minimum-Cost Seismic Retrofitting of Hysteretic Frames with Nonlinear Fluid Viscous Dampers. *Earthquake Engineering and Structural Dynamics*, **47**, 2958-3005.

[17] Golberg, D. (1989): *Genetic Algorithms in Search, Optimization and Machine Learning*, Addison-Wesley.

[18] Camp, C., Pezeshk, S., and Cao, G. (1998): Optimized Design of Two-Dimensional Structures Using a Genetic Algorithm. *Journal of Structural Engineering*, **124** (5), 551-559.

[19] FEMA (2011): Reducing the Risk of Nonstructural Earthquake Damage – A Practical Guide. *Report E-74 Federal Emergency Management Agency*, Washington, D.C.

[20] Steneker, P., Filiatrault, A., Wiebe, L., Konstantinidis, D. (Forthcoming): Integrated Structural-Nonstructural Performance-Based Seismic Design and Retrofit Optimization of Buildings. *Journal of Structural Engineering*, DOI: 10.1061/(ASCE)ST.1943-541X.0002680.

[21] Gupta, A., and Krawinkler, H. (1999): Seismic Demands for Performance Evaluation of Steel Moment Resisting Frame Buildings, *Stanford University*, *Report No. 132*, Stanford, CA.

[22] FEMA (2012): Seismic Performance Assessment of Buildings - Normative Quantity Estimating Tool. *Report P-58 Federal Emergency Management Agency*, **3.3**, Washington, D.C.

[23] Uniform Building Code (1994): Structural Engineering Design Provisions. **2**, *International Conference of Building Officials*, Lansing, MI.

[24] American Society of Civil Engineers (2016): Minimum Design Loads and Associated Criteria for Buildings and Other Buildings. *ASCE 7-16*, Reston, VA.

[25] American Institute of Steel Construction (2016): Seismic Provisions for Structural Steel Buildings *AISC 341-16*, Chicago, IL.

[26] McKenna, F., Fenves, G. L., and Scott, M. (2000): *Open System for Earthquake Engineering Simulation*. University of California Berkeley, CA.

[27] Ibarra, L., Medina, R., and Krawinkler, H. (2005): Strength demand issues relevant for the seismic design of moment-resisting frames. *Earthquake Spectra*, **21** (2), 415–439.

[28] Charney, F., and Pathak, R. (2008): Sources of Elastic Deformation in Steel Frame and Framed-Tube Buildings: Part 1: Simplified Subassemblage Models. *Journal of Constructional Steel Research*, **64** (1), 87–100.

[29] Baker, J. W. (2015): Efficient Analytical Fragility Function Fitting Using Dynamic Structural Analysis. *Earthquake Spectra*, **31** (1) 579–599.

[30] Baker, J. W., and Lee, C. (2017): An Improved Algorithm for Selecting Ground Motions to Match a Conditional Spectrum. *Journal of Earthquake Engineering*, **22** (4), 708-723.

[31] Pacific Earthquake Engineering Research Center (2013): PEER NGA-West2 Database. *Pacific Earthquake Engineering Research Center Report No. 2012/03*, Berkeley, CA.

[32] Khoo, H.-H., Clifton, C., Butterworth, J., MacRae, G., Gledhill, S., and Sidwell, G. (2012): Development of the Self-centering Sliding Hinge Joint with Friction Ring Springs. *Journal of Constructional Steel Research*, **78**, 201–211.

[33] Khoo, H. H., Clifton, C., Butterworth, J., and MacRae, G. (2013): Experimental Study of Full-scale Self-centering Sliding Hinge Joint Connections with Friction Ring Springs. *Journal of Earthquake Engineering*, **17** (7), 972–977.

[34] Filiatrault, A., Tremblay, R., and Kar, R. (2000): Performance Evaluation of Friction Spring Seismic Damper. *Journal of Structural Engineering*, **126**(4), 491-499.

[35] Black, C. J., Makris, N., and Aiken, I. D. (2004): Component Testing, Seismic Evaluation and Characterization of Buckling-Restrained Braces. *Journal of Structural Engineering*, **130** (6), 880-894.

[36] Christopoulos, C., and Filiatrault, A. (2006): *Principles of Passive Supplemental Damping and Seismic Isolation*, IUSS Press, Pavia, Italy.

[37] Soroushian, S., Zaghi, A., Maragakis, M., Echevarria, A., Tian, Y., Filiatrault, A., (2015): Analytical Seismic Fragility Analyses of Fire Sprinkler Piping Systems with Threaded Joints *Earthquake Spectra*, **31** (2), 1125-1155.

[38] Filiatrault, A., Kuan, S., Tremblay, R., (2004): Shake Table Testing of Bookcase-partition Wall Systems *Canadian Journal of Civil Engineering*, **31**, pp. 664-676.

[39] Behr, R. (2001): Architectural Glass for Earthquake-resistant Buildings, *Proceedings of the 7th international glass conference*, Tampere, Finland.

[40] Retamales, R., Davies, R., Masqueda, G., Filiatrault, A., (2013): Experimental Seismic Fragility of Cold-Formed Steel Framed Gypsum Partition Walls *Journal of Structural Engineering*, **139** (8), 1285-1293.

[41] Bull, D., (2011): Stairs and Access Ramps Between Floors in Multi-storey Buildings. *Report to the Royal Commission*, **1**, pp. 1-8.

[42] American Society of Civil Engineers. (2017): Seismic Evaluation and Retrofit of Existing Buildings. *ASCE 41-17*, Reston, VA.

[43] Shilling, J. and Wurtzebach, C. (2012): Is Value-Added and Opportunistic Real Estate Investing Beneficial? If So, Why? *Journal of Real Estate Research*, **34** (4), 429-461.

